



Published in final edited form as:

*Pain*. 2008 August 15; 138(1): . doi:10.1016/j.pain.2008.04.018.

## Regional brain activation in conscious, nonrestrained rats in response to noxious visceral stimulation

Zhuo Wang<sup>a,c</sup>, Sylvie Bradesi<sup>a,c</sup>, Jean-Michel I. Maarek<sup>d</sup>, Kevin Lee<sup>f</sup>, Wendy J. Winchester<sup>f</sup>, Emeran A. Mayer<sup>a,b,c</sup>, and Daniel P. Holschneider<sup>c,d,e,\*</sup>

<sup>a</sup>Center for the Neurobiology of Stress, Brain Research Institute, UCLA, Los Angeles, CA, USA

<sup>b</sup>Departments of Physiology, Psychiatry and Biobehavioral Sciences, Brain Research Institute, UCLA, Los Angeles, CA, USA

<sup>c</sup>VA GLA Healthcare System, Los Angeles, CA, USA

<sup>d</sup>Department of Biomedical Engineering, USC, Los Angeles, CA, USA

<sup>e</sup>Departments of Psychiatry and the Behavioral Sciences, Cell and Neurobiology, Neurology, USC, Los Angeles, CA, USA

<sup>f</sup>Neurology and GI Center of Excellence for Drug Discovery, GlaxoSmithKline, Harlow, UK

### Abstract

Preclinical drug development for visceral pain has largely relied on quantifying pseudoaffective responses to colorectal distension (CRD) in restrained rodents. However, the predictive value of changes in simple reflex responses in rodents for the complex human pain experience is not known. Male rats were implanted with venous cannulas and with telemetry transmitters for abdominal electromyographic (EMG) recordings. [<sup>14</sup>C]-iodoantipyrine was injected during noxious CRD (60 mmHg) in the awake, nonrestrained animal. Regional cerebral blood flow (rCBF)-related tissue radioactivity was quantified by autoradiography and analyzed in the three-dimensionally reconstructed brain by statistical parametric mapping. 60-mmHg CRD, compared with controls (0 mmHg) evoked significant increases in EMG activity ( $267 \pm 24\%$  vs.  $103 \pm 8\%$ ), as well as in behavioral pain score ( $77 \pm 6\%$  vs.  $3 \pm 3\%$ ). CRD elicited significant increases in rCBF as expected in sensory (insula, somatosensory cortex), and limbic and paralimbic regions (including anterior cingulate cortex and amygdala). Significant decreases in rCBF were seen in the thalamus, parabrachial nucleus, periaqueductal gray, hypothalamus and pons. Correlations of rCBF with EMG and with behavioral pain score were noted in the cingulate, insula, lateral amygdala, dorsal striatum, somatosensory and motor regions. Our findings support the validity of measurements of cerebral perfusion during CRD in the freely moving rat as a model of functional brain changes in human visceral pain. However, not all regions demonstrating significant group differences correlated with EMG or behavioral measures. This suggests that functional brain imaging captures more extensive responses of the central nervous system to noxious visceral distension than those identified by traditional measures.

## Keywords

Visceral pain; Abdominal pain; Nociception; Colorectal distension; Cerebral blood flow; Brain mapping

---

## 1. Introduction

The development of novel drugs for functional gastrointestinal disorders has been restricted by the lack of animal models with high predictive validity [45,46]. Current preclinical evaluation of drugs for visceral pain relies almost exclusively on measuring pseudoaffective responses to colorectal distension (CRD) [53] in restrained, and sometimes sedated rodents. Typically, electromyographic contraction of the abdominal muscles (visceromotor response, VMR) [12,24,58], or behavioral pain postures [65] are measured. In contrast, experimental medicine approaches to irritable bowel syndrome (IBS) evaluate patients' subjective perception of acutely induced rectosigmoidal pain. To capture more objective markers of the human visceral pain response, and to assess possible drug effects on this response, functional magnetic resonance imaging (fMRI) and positron emission tomography (PET) have been applied successfully to study the human brain response to aversive visceral stimuli [47]. In view of the multidimensional nature of the human pain experience, it is clear that pseudoaffective responses in rodents reflect only a small portion of the nociceptive response. To bridge the gap between preclinical and clinical models, and to evaluate the relevance of CRD animal models for human conditions, it is imperative to investigate whether or not CRD activates similar brain regions in animals as has been reported in humans.

To date, the majority of human studies in this field have used distension of the rectosigmoid colon [4,5,8,41,44,48,52,62], stomach [37,69], and esophagus [2,3,9,73]. Activation of the insular and dorsal anterior cingulate cortex (dACC) has been most consistently reported, with other brain regions, including the prefrontal cortex, thalamus and brainstem being reported in some, but not in other studies. Collectively, these findings are consistent with the notion that noxious visceral stimuli activate the *homeostatic afferent processing network*, a framework proposed to understand the processing of visceral, somatic, as well as emotional stimuli in the brain [17,18,47].

Research on brain responses to visceral stimuli in animals has relied predominantly on measuring c-fos expression [43,49,64,67]. Unlike human studies, c-fos studies typically require prolonged exposure of the animal to high-intensity visceral stimuli, which may lead to the integration of a variety of nonspecific stimuli over the duration of pain exposure, including acute sensitization of the visceral afferent system. Furthermore, analysis is often limited to a few selected brain regions, lacking the whole-brain level analysis achieved in human studies. Thus, it is not surprising that no consensus has emerged that allows comparison between rat c-fos data and human neuroimaging findings. Other region-specific analysis of neuronal responses to CRD has been carried out using in vivo electrophysiological recording technique [1,22]. Lazovic et al. conducted the only reported fMRI study in the rat CRD model [38]. However, the use of sedated animals complicated data interpretation.

We used the autoradiographic cerebral perfusion method to map brain activation in response to noxious CRD in conscious, unrestrained rats. Specifically, we sought to address the questions: (1) Are changes in regional cerebral blood flow (rCBF) induced by noxious CRD in the rat similar to rCBF changes reported in humans? (2) Does rCBF correlate with abdominal electromyography and behavioral pain measures?

## 2. Methods

### 2.1. Animals

Twenty-four adult, male Wistar rats (285–400 g at surgery) were randomized into two groups: distension and control ( $n = 12$  for each group). Rats were individually housed on a 12 h light/12 h dark cycle with free access to water and rodent chow. All experiments were conducted under a protocol approved by the Institutional Animal Care and Use Committee of the University of Southern California. Ethical guidelines for investigations of experimental pain in conscious animals provided by the Committee for Research and Ethical Issues of IASP were followed.

### 2.2. Surgical procedures

Animals were anesthetized (isoflurane 1.5% in 70% oxygen, 30% nitrous oxide). The right external jugular vein was cannulated with a 5 French silastic catheter, advanced into the superior vena cava. The port at the distal end of the catheter was tunneled subcutaneously and externalized dorsally in the region rostral to the scapula. Subsequently, a telemetry transmitter was implanted to measure abdominal EMG and locomotor activity. Such implants can be turned on and off with an external magnet, sending a radiofrequency signal of EMG activity, as well as locomotor activity counts to a receiver platform placed underneath the rat's cage. The body of the transmitter (TA10ETA-F20, Data Sciences Intl., St. Paul, MN) was implanted subcutaneously on the dorsum of the animal caudal to the scapula. A skin incision was made on the abdomen and electrodes of the transmitter were tunneled subcutaneously to the abdominal incision. Tips of the electrodes were bared, placed in parallel (0.5 cm apart), and stitched into the left external oblique musculature, just superior to the inguinal ligament [12]. The receiver platform was linked via a data exchange matrix to a computer. All animals were allowed to recover for seven days before cerebral perfusion and CRD experiments. The catheter was flushed every 2 days postoperatively to ensure patency (0.3 ml of 0.9% saline, followed by 0.1 ml of saline with 20 U/ml heparin). Prior to CRD and cerebral perfusion experiments, animals were habituated to an uninflated colorectal balloon and the experiment cage for 45 min. per day for 3 days.

### 2.3. Cerebral perfusion and CRD

The experimental setup allowed barostat-controlled (Distender Series II, G&J Electronics Inc., Toronto, Canada) application of CRD, telemetric recording of abdominal EMG, videotaping of behavior, as well as intravenous radiotracer infusion in conscious, nonrestrained animals (Fig. 1). Under light isoflurane anesthesia (1.5% isoflurane  $\times$  3 min), a flexible latex balloon (length: 6 cm) was inserted intra-anally such that its caudal end was 1 cm proximal to the anus. The silicon tubing connecting the balloon and the barostat was fixed to the base of the tail with adhesive tape and covered by a stainless steel spring for protection against animal biting. Animals were allowed to recover for 30 min. in the experiment cage, the floor of which was covered with bedding from the animal's home cage. In the meantime, a piece of tubing was filled with the radiotracer, [ $^{14}\text{C}$ ]-iodoantipyrine (125  $\mu\text{Ci}/\text{kg}$  in 300  $\mu\text{l}$  of 0.9% saline, American Radiolabelled Chemicals, St. Louis, MO). At the end of the recovery period, the tubing was connected to the animal's cannula on one end, and to a syringe filled with euthanasia agent (pento-barbital 75 mg/kg, 3 M potassium chloride) on the other. The animal was allowed to rest for 5 min. before receiving one episode of 60 mmHg, 60-s distension. Thirty-five seconds after the onset of distension, radiotracer was infused at 2.25 ml/min by a motorized pump, followed immediately by the euthanasia solution, which resulted in cardiac arrest within  $\sim 10$  s, a precipitous fall of arterial blood pressure, termination of brain perfusion, and death [28]. This 10-s time window provided the temporal resolution during which the distribution of rCBF-related tissue radioactivity (rCBF-TR) was mapped. Balloons in the control animals remained

uninflated (0 mmHg). EMG signals were telemetrically recorded and animal behavior was videotaped. Data were saved on a computer for offline analysis. The experimental cage was wiped with a cloth dampened with 1% ammonia between animals.

#### 2.4. Brain slicing and autoradiography

Brains were rapidly removed, flash frozen in dry ice/ methylbutane ( $-55^{\circ}\text{C}$ ) and embedded in OCT compound (Sakura Fintek Inc., Torrance, CA). Brains were subsequently sectioned on a cryostat (HM550 Series, Microm International GmbH, Walldorf, Germany) at  $-18^{\circ}\text{C}$  into 20- $\mu\text{m}$ -thick coronal slices, with an inter-slice spacing of 300  $\mu\text{m}$ . The sampling did not include brain stem and spinal cord. Slices were heat-dried on glass slides and exposed for 2 weeks at room temperature to Ektascan Diagnostic Film (Eastman Kodak Co., Rochester, NY). Images of brain sections were then illuminated on a voltage-stabilized lightbox with light diffuser (Northern Lights Illuminator, InterFocus Ltd., Linton, England), photographed with a Retiga 4000R charge-coupled device monochrome camera (QImaging, Surrey, Canada) equipped with a 60-mm AF Micro Nikkor lens (Nikon, Melville, NY), and digitized on an 8-bit gray scale through an ATI FireGL V3100 128 MB digitizing board and QCapture Pro 5.1 software (QImaging) on a computer.

#### 2.5. Abdominal EMG analysis

Electromyographic (EMG) signals were recorded telemetrically at a sampling rate of 1 kHz, digitized and stored on a computer with Dataquest ART 3.0 (Data Sciences Intl., St. Paul, MN). Waveforms were lowcut filtered at 20 Hz to eliminate movement interference [58] and full-wave rectified. To analyze the time course of EMG activity in response to CRD, each rat's rectified EMG signal was averaged over consecutive 1-s intervals for the 40 s period before (baseline) and 40 s after the onset of CRD. The latter 40 s included a final 5 s period in which the radiotracer infusion had begun but euthanasia had not been initiated. Averaged EMG signals were further normalized to the average of the 40-s baseline. Area under the curve (AUC) was calculated for the 40 s period after CRD onset. Control group (0 mmHg) data were analyzed in the same fashion at equivalent time points but in the absence of CRD. EMG responses were presented as group mean  $\pm$  SEM. EMG signals in two control rats were not recorded due to transmitter failure. The Student's *t*-test was used to test statistical significance ( $P < 0.05$ ). Pearson's test was used for correlation analysis (EMG vs. behavioral pain score,  $P < 0.05$ ).

#### 2.6. Behavioral analysis of nociception

Animal behavior was recorded with two digital camcorders placed horizontally at a  $90^{\circ}$  angle. Video was digitized and stored on a computer using the Observer XT software (Noldus Inc., Leesburg, VA), which was also used for off-line analysis of behavior. Postures indicative of visceral pain were defined as in Stam et al. [65]: arching (convex back and retraction of the abdomen from the floor) and stretching (whole body stretched out on floor). We quantified the cumulative duration during which the animal assumed either pain posture, and computed the percentage of time spent in pain postures during the first 40 s of CRD. In addition, for each animal locomotor activity counts were obtained from the telemetry recording over consecutive 1 sec. intervals and summed for the 40 s period after CRD onset. Data were presented as group means  $\pm$  SEM. The Student's *t*-test was used to test statistical significance ( $P < 0.05$ ).

#### 2.7. Functional brain mapping data analysis

rCBF-TR was quantified by autoradiography and analyzed on a whole-brain basis using statistical parametric mapping (SPM, version SPM2, Wellcome Centre for Neuroimaging, University College London, London, UK), a software package widely used to analyze

human brain imaging data [21]. Recently, we and others have developed and validated an adaptation of SPM for use in animal autoradiograph [29,40,57]. In preparation for the SPM analysis, a 3D reconstruction of each animal's brain was conducted using 57 serial coronal sections. Adjacent sections were aligned both manually and using TurboReg, an automated pixel-based registration algorithm. This algorithm registered each section sequentially to the previous section using a nonwarping geometric model that included rotations and translations (rigid-body transformation) and nearest-neighbor interpolation [66]. A typical reconstructed brain has ~2,750,000 voxels (voxel size:  $40 \times 40 \times 300 \mu\text{m}$ ). After 3D reconstruction, one "artifact free" brain was selected as reference and smoothed with a Gaussian kernel ( $\text{FWHM} = 3 \times \text{voxel dimension}$ ). All brains were spatially normalized to the smoothed reference brain. The spatial normalization consisted of applying a 12-parameter affine transformation followed by a nonlinear spatial normalization using 3D discrete cosine transforms. Normalized images were averaged to create a mean image, which was then smoothed to create the final rat brain template. Each original 3D reconstructed brain was then spatially normalized into a standard space defined by the template. A nonbiased, voxel-by-voxel analysis of whole-brain activation using SPM was used for the detection of significant changes in functional brain activation between rats exposed to CRD and controls. Global differences in the absolute amount of radiotracer delivered to the brain were adjusted in SPM for each animal by scaling the voxel intensities so that the mean intensity for each brain was the same (proportional scaling). We implemented a Student's *t*-test at each voxel, testing the null hypothesis that there was no effect of group. We chose to set a significance threshold  $P < 0.05$  for individual voxels within clusters of at least 100 contiguous voxels (extent threshold). To detect brain regions showing rCBF correlated with either pain measure, SPM analysis using EMG-AUC and pain score as individual covariate was run for the group of rats receiving 60-mmHg CRD. Significance level was set at  $P < 0.05$  for Pearson's correlation coefficient. Brain regions were identified using a rat brain atlas [59].

### 3. Results

Part of the results had previously been reported in abstract form [71].

#### 3.1. Abdominal EMG responses to noxious CRD

Application of a 60-mmHg CRD evoked significant VMRs, measured as abdominal EMG activity. The EMG activity remained elevated compared to controls during the entire 40 s period after CRD onset. The response was maximal at onset, declined over the first 20 s, and reached an elevated, downward sloping plateau level between 20 and 40 s period (Fig. 2A). Similar responses have been reported by others [58] and may reflect the contractile properties of the population of abdominal muscle fibers. EMG-AUC was computed for the 40 s period after the CRD onset and normalized to the 40 s baseline period before CRD. CRD evoked significant increase of EMG-AUC compared with 0-mmHg controls ( $267 \pm 24\%$  vs.  $103 \pm 8\%$ ,  $n = 12$  for CRD group,  $n = 10$  for control,  $P < 0.0001$ , Fig. 2B).

#### 3.2. Behavioral responses to noxious CRD

CRD at 60-mmHg evoked behavioral responses indicative of visceral nociception. Pain score was computed as percentage of time the animal spent in pain postures, defined as arching or stretching, during the 40 s period after CRD onset. Animals exposed to 60-mmHg distension spent  $77 \pm 6\%$  (vs.  $3 \pm 3\%$  in 0-mmHg controls,  $n = 12$  for each group,  $P < 0.0001$ , Fig. 2C) of time in pain postures, predominantly arching, whereas such postures were rarely observed in control animals in the corresponding time period. We did not observe other pain postures that have been reported such as writhing or squashing [65]. There was no significant group difference in total locomotor activity counts measured by

radio-telemetry (control rats  $8.4 \pm 2.9$  vs. CRD rats  $6.4 \pm 2.1$  counts,  $n = 10$  for control,  $n = 12$  for CRD group,  $P = 0.56$ ) during the 40 s of CRD.

### 3.3. Correlation between EMG response and behavioral pain score

In the group of rats exposed to 60-mmHg CRD, EMG-AUC and pain score showed trends of positive correlation without reaching statistical significance ( $n = 12$ ,  $R = 0.469$ ,  $P = 0.124$ , Pearson's correlation coefficient, Fig. 2D). Seven out of the twelve animals had a pain score of >90%, a ceiling effect that might have affected the results of the correlation analysis. The lack of significant correlation between EMG and the behavioral pain score suggests that while both measures may be responsive to increases in pain, they provide different information about the animal's response to the nociceptive stimulus.

### 3.4. Brain responses to noxious CRD

**3.4.1. Cerebral cortex**—Significant group differences in rCBF obtained by SPM analysis are shown in the form of significant  $T$ -score differences mapped onto selected coronal sections of the rat brain used for reference (Fig. 3). A comprehensive list of significant group differences is shown in Table 1 ( $n = 12$  for each group,  $P < 0.05$ ). Significant increases in rCBF included the dorsal anterior cingulate (dACC, Cg1), anterior and mid/posterior insular (I), primary and secondary motor (M1, M2), prelimbic (PrL), primary somatosensory (S1HL: hindlimb; S1Tr: trunk), secondary somatosensory (S2), temporal association (TeA), and auditory (Au) cortices. Significant clusters extended through the full thickness of the cortical layer. Bilateral significant increases whose clusters were noted mostly in the mid to outer cortical layer included the parietal (PtA: association area), primary somatosensory (S1FL: forelimb; S1BF: barrel field), primary visual cortex (V1). Though cortical activations noted in response to CRD in our study were bilateral, there was a clear lateralization, such that activations were larger in the left hemisphere.

**3.4.2. Subcortical regions**—Bilateral increases in rCBF included the dorsal caudate-putamen (CPu), amygdala (CeA: central; LaA: lateral), the amygdalostratial transition area (ASt), and inferior colliculus (IC), with left hemispheric activation exceeding right hemispheric activation. Decreases in rCBF included the lateral caudate-putamen, lateral hypothalamus (PLH: posterior; PeFLH: perifornical), parabrachial nucleus (PBN), periaqueductal gray (PAG), red nucleus (RN), parabrachial nucleus (PaR), reticular nucleus of the pons (PnC), substantia nigra (SN), superior colliculus (SC), and thalamus (PF: parafascicular; VPPC: parvicellular ventral posterior nucleus; Po: posterior; VM: ventromedial; VPL: ventral posterior lateral; VPM: ventral posterior medial). Left sided decreases in activation were noted in the posterior hippocampal CA1 region and trigeminal nucleus (Pr5VL: sensory, ventrolateral).

### 3.5. Correlations of rCBF vs. EMG and of rCBF vs. behavioral pain score

We performed regression using EMG-AUC and pain score as individual covariate in SPM analysis for the group of rats receiving 60-mmHg CRD. rCBF showed significant positive correlation ( $n = 12$ ,  $P < 0.05$ , Pearson's correlation coefficient) with both EMG and behavioral pain measures in the dACC, the insular cortex (anterior, posterior), secondary motor cortex, primary somatosensory cortex of the hindlimbs, forelimbs, trunk and barrel fields, lateral amygdala, and dorsal caudate-putamen. rCBF was significantly and negatively correlated with EMG and pain score in the PAG.

Some discrepancies were noted between the group comparison (CRD vs. controls) and the correlations of rCBF with EMG, and rCBF with pain score. Compared to non-distended controls, CRD was associated with significant activation in the central nucleus of the amygdala, even though there was no significant correlation in this region with EMG or pain

score. A significant positive correlation was seen in the anterior basolateral amygdala for the rCBF–EMG correlation, but not for the rCBF–pain score correlation or the group comparison. In the lateral orbital cortex, a significant positive correlation was noted for both rCBF–EMG and rCBF–pain score correlations, but not for the group comparison. Group differences in prelimbic cortex showed a significant positive correlation of rCBF with EMG, but not with pain score.

## 4. Discussion

We show that acute noxious CRD in freely moving rats is associated with changes in rCBF in brain regions previously reported to be responsive to similar stimuli in humans. CRD is also associated with reflex and complex behavioral responses, which correlated with several of the activated brain regions. To our knowledge, this is the first report of perfusion mapping in freely moving rats during the elicitation of visceral pain.

### 4.1. Are there changes in rCBF induced by noxious CRD in the rat similar to rCBF changes reported in human studies?

**4.1.1. Activations**—In our study, CRD evoked bilateral activation in the PrL, dACC and anterior and mid/posterior insula, as well as S1, S2, M1, and M2. These results are in close alignment with prior results reported in normal human subjects. In particular, human studies have identified the insular cortex as the single most consistently activated brain region to CRD [4,5,19,27,31,41,48,52, 62,63], with the anterior insula proposed to provide the substrate for a subjective evaluation of the interoceptive state [17]. A majority of studies have also reported activation of the dACC [4,5,27,31,41,44,52, 62,63], S1/S2 [4,8,27,31,41,63] and prefrontal cortical regions [4,8,27,31,44,52,62,63] in response to CRD.

The increased activation in motor cortex in response to CRD was unlikely due to locomotion as activity counts were extremely low during the period of distention, and without significant group differences. Neuroimaging studies in humans have associated abdominal contractions with activation of the superolateral precentral gyrus (lateral portion of motor cortex) and premotor and supplemental motor cortex [10,72]. In addition, focal stimulation of these areas, either magnetically or electrically, evokes abdominal straining [15,20,34].

Activation in many cortical areas was seen throughout the full thickness of the cortex (including dACC, insula, M1, M2, PrL, S1HL, S1Tr, S2, Au, Ect, TeA and V2). Supragranular layers (especially layer III) establish cortico-cortical connections, whereas most of the connectivity established by the deeper, infragranular layers (layers V and VI) are of the cortico-fugal type [33]. This suggests that visceral noxious stimulation not only produces greater activation of cortical neurons, but also produces a powerful output from localized cortical areas to subcortical structures. Traub et al., examining c-fos expression in rats after exposure to CRD, have noted similar findings: whereas restrained control animals showed activation of c-fos only in the supragranular cortical layers, both the supragranular and infragranular layers expressed c-fos after CRD [67]. Cortical activations noted in our study were more widespread than those reported in humans. This difference may be attributable to species differences and to difference in the magnitude of the CRD. In the current study, the colon was distended to 60 mmHg (associated with EMG changes), while in human studies, visceral stimuli of less than 40 mmHg are typically applied, resulting in subjective reports of pain or discomfort, rather than muscle contraction.

Rats exposed to CRD compared to controls also showed activation in several subcortical regions, including the central (CeA) and lateral (LaA) aspects of the amygdala and the amygdalostratial transition area (ASt). The amygdala plays a key role in emotional

responses to various sensory stimuli [39,51], including nociceptive stimuli [54]. It receives nociceptive information through the spino-parabrachio-amygdaloid pain pathway, which connects the spinal cord and the pontine parabrachial area (PBN) with the CeA [6,7]. Nociceptive information may also reach the amygdala as a collateral branch of the spinothalamic path, or as a direct projection from the spinal cord [14]. Polymodal sensory information reaches the CeA from thalamic and cortical areas through connections with the lateral and basolateral amygdaloid nuclei [39,60]. The latero-capsular part of the CeA is now defined as the ‘nociceptive amygdala’ because of its high content of nociceptive neurons [7,55,56]. Chemical stimulation of the CeA enhances visceromotor responses to CRD in rats and causes the sensitization of spinal neurons with visceral input [24,61]. Interestingly, it has been suggested that an LaA–ASt pathway may be involved in the processing of emotional significance and rapid reflexive responses during fear-induced behavior [30,70].

Prior studies in rats have shown activation of the amygdala by CRD, as measured by increases in c-fos expression [38,49,67] or fMRI activation [38], while others have reported no difference between CRD and sham distention [43]. In healthy human subjects, amygdala activation has been reported in response to gastric dis-tension [42], whereas decrease in activation has been reported in response to CRD (at least in female subjects) [5,11,52,63], though these studies have not provided information on subnuclei. In patients with IBS both increased activation [11] and no change [5,52,63] have been reported in response to CRD. The discrepancy may be attributable to differences in the experimental design and differences in CRD delivery parameters. The amygdala’s response to visceral pain may also be dynamic, as is its response to conditioned fear [13,35]. Preliminary fMRI results from humans suggest that amygdala activation is only seen during the early phase of noxious stimulation, and that activation is transient [36]. In addition, the persistent activation of the amygdala in the current study may reflect a stronger emotional component in the rats due to higher CRD inflation pressures.

Significant increases in rCBF were seen in dorsal caudate-putamen. Several human studies also showed activation in the striatum in response to CRD [5,52,63] or gastric distention [37] in normal subjects. Neuroanatomical evidence suggests that nociceptive information may reach the basal ganglia through several afferent sources including the medial and posterior thalamus, amygdala, PBN area, dorsal raphe nucleus, as well as cortical regions. There is evidence to implicate the basal ganglia in pain processing and modulation, including the encoding of pain intensity, affective and cognitive aspects, sensory gating of nociceptive information to higher motor areas, and modulation of pain behavior [16,54].

**4.1.2. Decreases in activation**—Significant decreases in activation were prominent in subcortical regions that are targets of the spinothalamic track (STT), including the VPL and Po, as well as target areas of the spinoreticular and spinomesencephalic afferents (including the PBN and PAG). In addition, significant decreases in activation were noted in the PF and VPPC. The PF has been proposed to serve a role in sensory awareness and limbic–motor functions [68]. The main function of the VPPC has been the transfer of gustatory and visceral information to the insular cortices [25]. Major ascending inputs to the VPPC are derived from the PBN. The VPPC, in turn, projects to the LaA and CeA, the amygdalostratial transition area, and to more rostral areas of the striatum (typically ventral, though in our study we observed more dorsal activation). Cortical projections are primarily directed at the insula (mostly posterior), which, in turn, sends reciprocal efferents back to the VPPC. This pattern of widespread decrease in thalamic activation is consistent with the proposal that neurons of the sensory cortex are capable of inhibitory control over the thalamo-cortical units of STT origin that project to them [23]. Such sensory cortical inhibition has been proposed to function in the ‘stabilization’ of afferent volleys in order to



strengthen the signal-to-noise ratio of particular afferent volleys and facilitate discrimination of sensory input [23,50]. There is also evidence suggesting that network inhibition within the thalamus, in particular between VPL and the reticular thalamic nucleus, plays a role in the control of visceral nociception [32].

#### 4.2. Does the activity in these regions correlate with EMG and behavioral pain measures?

We performed correlational analysis in SPM using EMG-AUC and pain score as individual covariate for the group of rats receiving 60-mmHg CRD. rCBF showed positive correlation with both EMG and pain score in the dACC, I, M2, S1, lateral orbital cortices, as well as in the lateral amygdala and dorsal caudate-putamen. rCBF in the PrL was positively correlated with EMG, but not pain score.

Human neuroimaging studies have identified the dACC [48,62] and caudate [26] as regions showing the most significant positive correlation of rCBF with patient's reported pain intensity during noxious CRD. Trends of positive correlation have been observed in the prefrontal cortex [26,62], thalamus [62], striatum [62], and supplementary motor cortex [26]. That EMG and behavioral pain score both correlated with activation of the dACC in CRD rats validated, in part, the relevance of these pain measures.

The clusters showing significant correlations with either EMG or pain score were noticeably smaller than those showing group differences in rCBF within a given region. Furthermore, not all brain regions that showed group differences correlated with EMG or pain score. These suggest that EMG and behavioral measures are likely to reflect only part of the animal's response to the noxious visceral stimulus.

### 5. Summary and conclusions

Many of the regions that have shown significant rCBF changes during noxious visceral stimuli in humans demonstrated significant changes in the rat CRD model. Our findings support the validity of measurements of cerebral perfusion during CRD in the rat as a model of functional brain changes in human visceral pain. Functional brain mapping in rodents may therefore be a useful tool for preclinical evaluation of candidate drugs, the results of which may predict similar changes in humans. Future studies will have to address the predictive validity of this model.

### Acknowledgments

The research was supported by a Grant from GlaxoSmithKline and by the Animal Models Core of the Center for Neurobiology of Stress (NCCAM R24 AT002681). K. Lee and W.J. Winchester are employees of GlaxoSmithKline.

### References

1. Al-Chaer ED, Lawand NB, Westlund KN, Willis WD. Visceral nociceptive input into the ventral posterolateral nucleus of the thalamus: a new function for the dorsal column pathway. *J Neurophysiol.* 1996; 76:2661–74. [PubMed: 8899636]
2. Aziz Q, Andersson JL, Valind S, Sundin A, Hamdy S, Jones AK, et al. Identification of human brain loci processing esophageal sensation using positron emission tomography. *Gastroenterology.* 1997; 113:50–9. [PubMed: 9207261]
3. Aziz Q, Thompson DG, Ng VW, Hamdy S, Sarkar S, Brammer MJ, et al. Cortical processing of human somatic and visceral sensation. *J Neurosci.* 2000; 20:2657–63. [PubMed: 10729346]
4. Baciú MV, Bonaz BL, Papillon E, Bost RA, Le Bas JF, Fournet J, et al. Central processing of rectal pain: a functional MR imaging study. *AJNR Am J Neuroradiol.* 1999; 20:1920–4. [PubMed: 10588119]

5. Berman SM, Naliboff BD, Suyenobu B, Labus JS, Stains J, Bueller JA, et al. Sex differences in regional brain response to aversive pelvic visceral stimuli. *Am J Physiol Regul Integr Comp Physiol.* 2006; 291:R268–76. [PubMed: 16614061]
6. Bernard JF, Besson JM. The spino(trigemino)pontoamygdaloid pathway: electrophysiological evidence for an involvement in pain processes. *J Neurophysiol.* 1990; 63:473–90. [PubMed: 2329357]
7. Bernard JF, Bester H, Besson JM. Involvement of the spinoparabrachio- amygdaloid and -hypothalamic pathways in the autonomic and affective emotional aspects of pain. *Prog Brain Res.* 1996; 107:243–55. [PubMed: 8782523]
8. Bernstein CN, Frankenstein UN, Rawsthorne P, Pitz M, Summers R, McIntyre MC. Cortical mapping of visceral pain in patients with GI disorders using functional magnetic resonance imaging. *Am J Gastroenterol.* 2002; 97:319–27. [PubMed: 11866268]
9. Binkofski F, Schnitzler A, Enck P, Frieling T, Posse S, Seitz RJ, et al. Somatic and limbic cortex activation in esophageal distention: a functional magnetic resonance imaging study. *Ann Neurol.* 1998; 44:811–5. [PubMed: 9818938]
10. Blok BF, Sturms LM, Holstege G. A PET study on cortical and subcortical control of pelvic floor musculature in women. *J Comp Neurol.* 1997; 389:535–44. [PubMed: 9414011]
11. Bonaz B, Baci M, Papillon E, Bost R, Gueddah N, Le Bas JF, et al. Central processing of rectal pain in patients with irritable bowel syndrome: an fMRI study. *Am J Gastroenterol.* 2002; 97:654–61. [PubMed: 11926209]
12. Bradesi S, Schwetz I, Ennes HS, Lamy CM, Ohning G, Fanselow M, et al. Repeated exposure to water avoidance stress in rats: a new model for sustained visceral hyperalgesia. *Am J Physiol Gastrointest Liver Physiol.* 2005; 289:G42–53. [PubMed: 15746211]
13. Buchel C, Morris J, Dolan RJ, Friston KJ. Brain systems mediating aversive conditioning: an event-related fMRI study. *Neuron.* 1998; 20:947–57. [PubMed: 9620699]
14. Burstein R, Potrebic S. Retrograde labeling of neurons in the spinal cord that project directly to the amygdala or the orbital cortex in the rat. *J Comp Neurol.* 1993; 335:469–85. [PubMed: 8227531]
15. Carr LJ, Harrison LM, Stephens JA. Evidence for bilateral innervation of certain homologous motoneurone pools in man. *J Physiol.* 1994; 475:217–27. [PubMed: 8021829]
16. Chudler EH, Dong WK. The role of the basal ganglia in nociception and pain. *Pain.* 1995; 60:3–38. [PubMed: 7715939]
17. Craig AD. How do you feel? Interoception: the sense of the physiological condition of the body. *Nat Rev Neurosci.* 2002; 3:655–66. [PubMed: 12154366]
18. Craig AD. Pain mechanisms: labeled lines versus convergence in central processing. *Annu Rev Neurosci.* 2003; 26:1–30. [PubMed: 12651967]
19. Eickhoff SB, Lotze M, Wietek B, Amunts K, Enck P, Zilles K. Segregation of visceral and somatosensory afferents: an fMRI and cytoarchitectonic mapping study. *Neuroimage.* 2006; 31:1004–14. [PubMed: 16529950]
20. Foerster, O. Motorische Felder und Bahnen. In: Bumke, O.; Foerster, O., editors. *Handbuch der neurologie.* Vol. 6. Berlin: Springer; 1936. p. 50-1.
21. Friston KJ, Frith CD, Liddle PF, Frackowiak RS. Comparing functional (PET) images: the assessment of significant change. *J Cereb Blood Flow Metab.* 1991; 11:690–9. [PubMed: 2050758]
22. Gao J, Wu X, Owyang C, Li Y. Enhanced responses of the anterior cingulate cortex neurones to colonic distension in viscerally hypersensitive rats. *J Physiol.* 2006; 570:169–83. [PubMed: 16239277]
23. Giordano, J. The Neuroscience of pain and analgesia. In: Boswell, MV.; Cole, BE., editors. *Weiner's pain management: a practical guide for clinicians.* Boca Raton, FL: CRC Press; 2006. p. 15-34.
24. Greenwood-Van Meerveld B, Gibson M, Gunter W, Shepard J, Foreman R, Myers D. Stereotaxic delivery of corticosterone to the amygdala modulates colonic sensitivity in rats. *Brain Res.* 2001; 893:135–42. [PubMed: 11223001]
25. Groenewegen, HJ.; Witter, MP. Thalamus. In: Paxinos, G., editor. *The rat nervous system.* San Diego: Elsevier Academic Press; 2004. p. 407-53.

26. Hamaguchi T, Kano M, Rikimaru H, Kanazawa M, Itoh M, Yanai K, et al. Brain activity during distention of the descending colon in humans. *Neurogastroenterol Motil.* 2004; 16:299–309. [PubMed: 15198652]
27. Hobday DI, Aziz Q, Thacker N, Hollander I, Jackson A, Thompson DG. A study of the cortical processing of ano-rectal sensation using functional MRI. *Brain.* 2001; 124:361–8. [PubMed: 11157563]
28. Holschneider DP, Maarek JM, Harimoto J, Yang J, Scremin OU. An implantable bolus infusion pump for use in freely moving, nontethered rats. *Am J Physiol Heart Circ Physiol.* 2002; 283:H1713–9. [PubMed: 12234827]
29. Holschneider DP, Yang J, Sadler TR, Nguyen PT, Givrad TK, Maarek JM. Mapping cerebral blood flow changes during auditory-cued conditioned fear in the nontethered, nonrestrained rat. *Neuroimage.* 2006; 29:1344–58. [PubMed: 16216535]
30. Jolkkonen E, Pikkarainen M, Kemppainen S, Pitkanen A. Interconnectivity between the amygdaloid complex and the amygdalostriatal transition area: a PHA-L study in rat. *J Comp Neurol.* 2001; 431:39–58. [PubMed: 11169989]
31. Kern MK, Jaradeh S, Arndorfer RC, Jesmanowicz A, Hyde J, Shaker R. Gender differences in cortical representation of rectal distension in healthy humans. *Am J Physiol Gastrointest Liver Physiol.* 2001; 281:G1512–23. [PubMed: 11705757]
32. Kim D, Park D, Choi S, Lee S, Sun M, Kim C, et al. Thalamic control of visceral nociception mediated by T-type Ca<sup>2+</sup> channels. *Science.* 2003; 302:117–9. [PubMed: 14526084]
33. Kolb, B. *The cerebral cortex of the rat.* Cambridge, MA: MIT Press; 1990.
34. Krause, F. *Chirurgie des Gehirns und Ruckenmarks nach eigenen Erfahrungen.* Berlin: Urban and Schwarzenberg; 1911.
35. LaBar KS, Gatenby JC, Gore JC, LeDoux JE, Phelps EA. Human amygdala activation during conditioned fear acquisition and extinction: a mixed-trial fMRI study. *Neuron.* 1998; 20:937–45. [PubMed: 9620698]
36. Labus, JS.; Mayer, EA.; Kilkens, TO.; Evers, EA.; Brummer, RM.; Backes, WH., et al. Acute tryptophan depletion (ATD) alters brain responses to aversive visceral stimulation in healthy women. *American college of neuropsychopharmacology 46th annual meeting program book; FL: Boca Raton.* 2007. p. 193
37. Ladabaum U, Minoshima S, Hasler WL, Cross D, Chey WD, Owyang C. Gastric distention correlates with activation of multiple cortical and subcortical regions. *Gastroenterology.* 2001; 120:369–76. [PubMed: 11159877]
38. Lazovic J, Wrzos HF, Yang QX, Collins CM, Smith MB, Norgren R, et al. Regional activation in the rat brain during visceral stimulation detected by c-fos expression and fMRI. *Neurogastroenterol Motil.* 2005; 17:548–56. [PubMed: 16078944]
39. LeDoux JE. Emotion circuits in the brain. *Annu Rev Neurosci.* 2000; 23:155–84. [PubMed: 10845062]
40. Lee JS, Ahn SH, Lee DS, Oh SH, Kim CS, Jeong JM, et al. Voxel-based statistical analysis of cerebral glucose metabolism in the rat cortical deafness model by 3D reconstruction of brain from autoradiographic images. *Eur J Nucl Med Mol Imaging.* 2005; 32:696–701. [PubMed: 15747156]
41. Lotze M, Wietek B, Birbaumer N, Ehrhardt J, Grodd W, Enck P. Cerebral activation during anal and rectal stimulation. *Neuroimage.* 2001; 14:1027–34. [PubMed: 11697934]
42. Lu CL, Wu YT, Yeh TC, Chen LF, Chang FY, Lee SD, et al. Neuronal correlates of gastric pain induced by fundus distension: a 3T-fMRI study. *Neurogastroenterol Motil.* 2004; 16:575–87. [PubMed: 15500514]
43. Martinez V, Wang L, Tache Y. Proximal colon distension induces Fos expression in the brain and inhibits gastric emptying through capsaicin-sensitive pathways in conscious rats. *Brain Res.* 2006; 1086:168–80. [PubMed: 16626641]
44. Mayer EA, Berman S, Suyenobu B, Labus J, Mandelkern MA, Naliboff BD, et al. Differences in brain responses to visceral pain between patients with irritable bowel syndrome and ulcerative colitis. *Pain.* 2005; 115:398–409. [PubMed: 15911167]
45. Mayer EA, Bradesi S, Chang L, Spiegel BM, Bueller JA, Naliboff BD. Functional GI disorders: from animal models to drug development. *Gut.* 2008; 57:384–404. [PubMed: 17965064]

46. Mayer EA, Collins SM. Evolving pathophysiologic models of functional gastrointestinal disorders. *Gastroenterology*. 2002; 122:2032–48. [PubMed: 12055608]
47. Mayer EA, Naliboff BD, Craig AD. Neuroimaging of the brain-gut axis: from basic understanding to treatment of functional GI disorders. *Gastroenterology*. 2006; 131:1925–42. [PubMed: 17188960]
48. Mertz H, Morgan V, Tanner G, Pickens D, Price R, Shyr Y, et al. Regional cerebral activation in irritable bowel syndrome and control subjects with painful and nonpainful rectal distention. *Gastroenterology*. 2000; 118:842–8. [PubMed: 10784583]
49. Monnikes H, Ruter J, König M, Grote C, Kobelt P, Klapp BF, et al. Differential induction of c-fos expression in brain nuclei by noxious and non-noxious colonic distension: role of afferent C-fibers and 5-HT<sub>3</sub> receptors. *Brain Res*. 2003; 966:253–64. [PubMed: 12618348]
50. Montero VM. Amblyopia decreases activation of the corticogeniculate pathway and visual thalamic reticularis in attentive rats: a 'focal attention' hypothesis. *Neuroscience*. 1999; 91:805–17. [PubMed: 10391464]
51. Nakagawa T, Katsuya A, Tanimoto S, Yamamoto J, Yamauchi Y, Minami M, et al. Differential patterns of c-fos mRNA expression in the amygdaloid nuclei induced by chemical somatic and visceral noxious stimuli in rats. *Neurosci Lett*. 2003; 344:197–200. [PubMed: 12812839]
52. Naliboff BD, Derbyshire SW, Munakata J, Berman S, Mandelkern M, Chang L, et al. Cerebral activation in patients with irritable bowel syndrome and control subjects during rectosigmoid stimulation. *Psychosom Med*. 2001; 63:365–75. [PubMed: 11382264]
53. Ness TJ, Gebhart GF. Colorectal distension as a noxious visceral stimulus: physiologic and pharmacologic characterization of pseudoaffective reflexes in the rat. *Brain Res*. 1988; 450:153–69. [PubMed: 3401708]
54. Neugebauer V. Subcortical processing of nociceptive information: basal ganglia and amygdala. In: Cervero, F.; Troels, S.J., editors. *Pain, handbook of clinical neurology*. Vol. 81. Amsterdam, The Netherlands: Elsevier; 2006. p. 141–58.
55. Neugebauer V, Li W. Differential sensitization of amygdala neurons to afferent inputs in a model of arthritic pain. *J Neurophysiol*. 2003; 89:716–27. [PubMed: 12574449]
56. Neugebauer V, Li W. Processing of nociceptive mechanical and thermal information in central amygdala neurons with knee-joint input. *J Neurophysiol*. 2002; 87:103–12. [PubMed: 11784733]
57. Nguyen PT, Holschneider DP, Maarek JM, Yang J, Mandelkern MA. Statistical parametric mapping applied to an autoradiographic study of cerebral activation during treadmill walking in rats. *Neuroimage*. 2004; 23:252–9. [PubMed: 15325372]
58. Nijssen MJ, Ongaene NG, Coulie B, Meulemans AL. Telemetric animal model to evaluate visceral pain in the freely moving rat. *Pain*. 2003; 105:115–23. [PubMed: 14499427]
59. Paxinos, G.; Watson, C. *The rat brain in stereotaxic coordinates*. New York: Elsevier Academic Press; 2005.
60. Pitkanen A, Savander V, LeDoux JE. Organization of intra-amygdaloid circuitries in the rat: an emerging framework for understanding functions of the amygdala. *Trends Neurosci*. 1997; 20:517–23. [PubMed: 9364666]
61. Qin C, Greenwood-Van Meerveld B, Foreman RD. Visceromotor and spinal neuronal responses to colorectal distension in rats with aldosterone onto the amygdala. *J Neurophysiol*. 2003; 90:2–11. [PubMed: 12634272]
62. Silverman DH, Munakata JA, Ennes H, Mandelkern MA, Hoh CK, Mayer EA. Regional cerebral activity in normal and pathological perception of visceral pain. *Gastroenterology*. 1997; 112:64–72. [PubMed: 8978344]
63. Song GH, Venkatraman V, Ho KY, Chee MW, Yeoh KG, Wilder-Smith CH. Cortical effects of anticipation and endogenous modulation of visceral pain assessed by functional brain MRI in irritable bowel syndrome patients and healthy controls. *Pain*. 2006; 126:79–90. [PubMed: 16846694]
64. Stam R, Ekkelenkamp K, Frankhuijzen AC, Bruijnzeel AW, Akkermans LM, Wiegant VM. Long-lasting changes in central nervous system responsiveness to colonic distension after stress in rats. *Gastroenterology*. 2002; 123:1216–25. [PubMed: 12360483]

65. Stam R, van Laar TJ, Wiegant VM. Physiological and behavioural responses to duodenal pain in freely moving rats. *Physiol Behav.* 2004; 81:163–9. [PubMed: 15059696]
66. Thevenaz P, Ruttimann UE, Unser M. A pyramid approach to subpixel registration based on intensity. *IEEE Trans Image Process.* 1998; 7:27–41. [PubMed: 18267377]
67. Traub RJ, Silva E, Gebhart GF, Solodkin A. Noxious colorectal distention induced-c-Fos protein in limbic brain structures in the rat. *Neurosci Lett.* 1996; 215:165–8. [PubMed: 8899739]
68. Van der Werf YD, Witter MP, Groenewegen HJ. The intralaminar and midline nuclei of the thalamus. Anatomical and functional evidence for participation in processes of arousal and awareness. *Brain Res Brain Res Rev.* 2002; 39:107–40. [PubMed: 12423763]
69. Vandenberg J, Dupont P, Fischler B, Bormans G, Persoons P, Janssens J, et al. Regional brain activation during proximal stomach distention in humans: a positron emission tomography study. *Gastroenterology.* 2005; 128:564–73. [PubMed: 15765391]
70. Wang C, Kang-Park MH, Wilson WA, Moore SD. Properties of the pathways from the lateral amygdal nucleus to basolateral nucleus and amygdalostriatal transition area. *J Neurophysiol.* 2002; 87:2593–601. [PubMed: 11976395]
71. Wang Z, Bradesi S, Maarek JMI, Lee K, Winchester WJ, Mayer EA, et al. Functional brain activation and visceral pain measurements in response to colorectal distension in unrestrained conscious rats. *Gastroenterology.* 2007; 132:A-717.
72. Woolsey CN, Erickson TC, Gilson WE. Localization in somatic sensory and motor areas of human cerebral cortex as determined by direct recording of evoked potentials and electrical stimulation. *J Neurosurg.* 1979; 51:476–506. [PubMed: 479934]
73. Yaguez L, Coen S, Gregory LJ, Amaro E Jr, Altman C, Brammer MJ, et al. Brain response to visceral aversive conditioning: a functional magnetic resonance imaging study. *Gastroenterology.* 2005; 128:1819–29. [PubMed: 15940617]

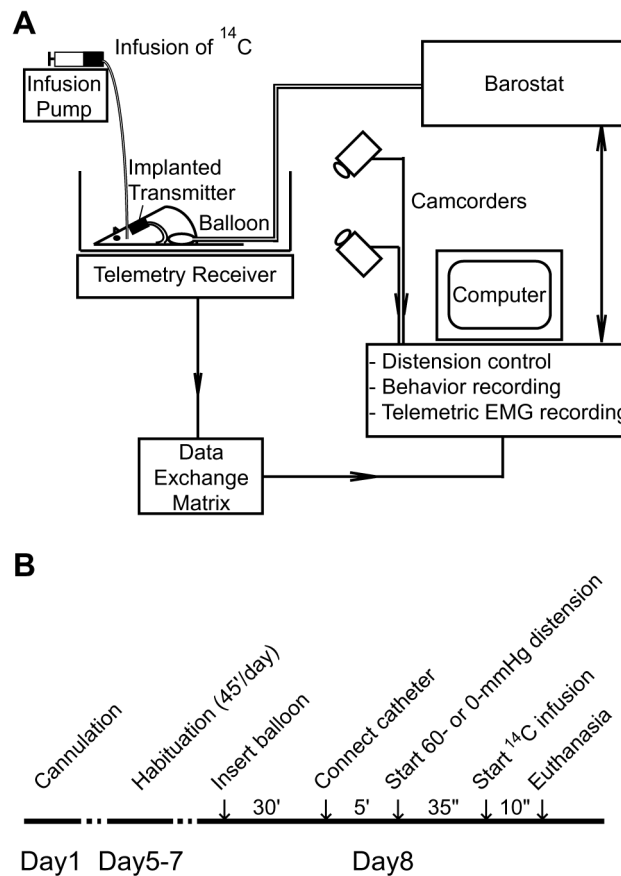


**Fig. 1.** Experimental setup and protocol. (A) The setup has four major components: (1) a barostat that controls inflation of the colorectal balloon; (2) a radio-telemetry system that records abdominal EMG through an implanted transmitter; (3) two digital camcorders that record animal behavior from front and side for behavior-based analysis of pain; (4) an infusion pump that controls intravenous infusion of radiotracer. Data are collected and stored on a computer for offline analysis. (B) Experimental protocol.

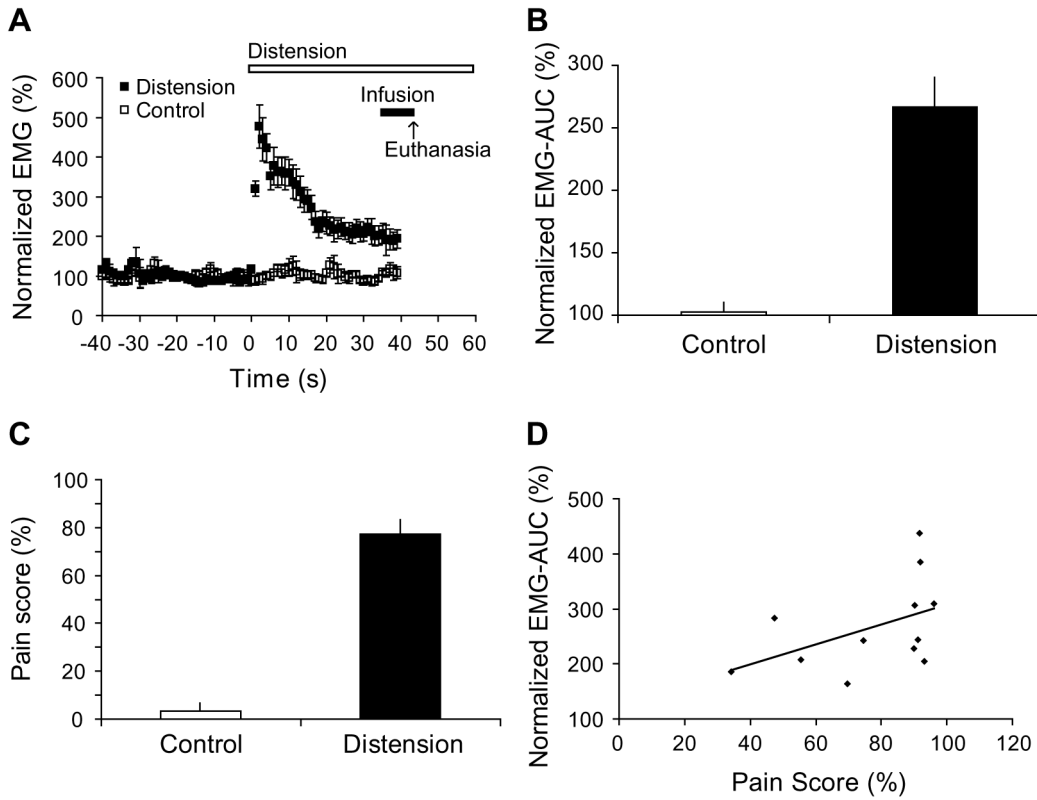


**Fig. 2.** EMG and behavioral responses to 60-mmHg colorectal distension. (A) Time course of EMG activity 40 s before (baseline) and 40 s after the onset of colorectal distension (CRD). Each data point represents group average of mean amplitude of rectified EMG over a 1-s interval. Data are normalized to average baseline amplitude (defined as 100%). (B) CRD evoked significant increase in EMG activity compared with 0-mmHg controls ( $267 \pm 24\%$  vs.  $103 \pm 8\%$ ,  $AUC \pm SEM$ ,  $n = 12$  for distension group,  $n = 10$  for control,  $P < 0.0001$ ). Area under curve (EMG-AUC) was computed over the 40 s period after CRD onset and normalized to baseline. (C) CRD evoked significant behavioral responses indicative of visceral pain ( $77 \pm 6\%$  at 60-mmHg vs.  $3 \pm 3\%$  at 0 mmHg,  $n = 12$  for each group,  $P < 0.0001$ ). Pain score was computed as the percentage of time the animal spent in postures indicative of visceral pain during the 40 s period after CRD onset. (D) Correlation between EMG-AUC and pain score in the group of animals exposed to 60-mmHg distension ( $n = 12$ ). EMG-AUC and pain score showed trends of positive correlation without reaching statistical significance ( $R = 0.469$ ,  $P = 0.124$ , Pearson's correlation coefficient).

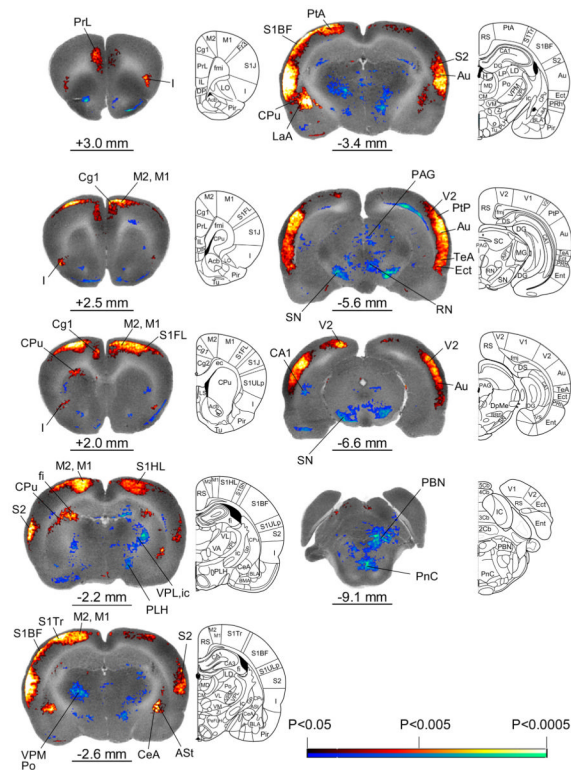


**Fig. 3.**

Changes in regional cerebral blood flow related tissue radioactivity in rats in response to 60-mmHg colorectal distension compared to 0-mmHg controls. Depicted is a selection of representative coronal slices (anterior–posterior coordinates relative to the bregma). Color-coded overlays show statistically significant positive (red) and negative (blue) differences of the 60-mmHg distension group compared to 0-mmHg controls ( $n = 12$  each group,  $P < 0.05$  at the voxel level, cluster  $> 100$  contiguous voxels). Line drawings have been adapted from those from the Paxinos and Watson (2005) rat atlas [59]: ASt (amygdalostratial transition area), Au (auditory cortex), CA1 (hippocampus CA1 region), CeA (central n. of the amygdala), Cg1 (cingulate cortex area 1), CPu (caudate-putamen), I (insula), ic (internal capsule), Ect (ectorhinal cortex), LaA (lateral amygdala n.), M1, M2 (primary, secondary motor cortex), MD (medial thalamic n.), PAG (periaqueductal gray), PBN (parabrachial n.), PeFLH (perifornical part of the lateral hypothalamus), PF (parafascicular thalamus), Pn (Pons), PrL (prelimbic cortex), Po (posterior thalamic n.), PtA (parietal association area), RN (red n.), S1BF (primary somatosensory cortex, barrel field), S1FL (primary somatosensory cortex, forelimb), S1HL (primary somatosensory cortex, hindlimb), S2 (secondary somatosensory cortex), SC (superior colliculus), SN (substantia nigra), TeA (temporal association cortex), V1, V2 (primary, secondary visual cortex), VPL, VPM (ventral posterior lateral, ventral posterior medial thalamic n.). The left side of each coronal section represents the left side of the brain of the animal. Rat brain atlas figures were reproduced with modification from Paxinos and Watson [59] with permission.



**Table 1**

Regions showing statistically significant differences of functional brain activation during 60-mmHg colorectal distension compared to 0-mmHg controls

<b>Brain region</b>	<b>Left/right</b>
<i>Cerebral cortex</i>	
Auditory (Au)	+/+ <sup>a</sup>
Cingulate, anterior dorsal (Cg1, dACC)	+/+ <sup>a</sup>
Ectorhinal (Ect)	+/+
Insular (I), anterior	+/+
Insular (I), mid/posterior	+/+ <sup>a</sup>
Motor, primary, secondary (M1, M2)	+/+ <sup>a</sup>
Parietal, association, posterior (PtA, PtP)	+/+
Prelimbic (PrL)	+/+
Somatosensory, primary, barrel field (S1BF)	+/+
Somatosensory, primary, forelimb (S1FL)	+/+
Somatosensory, primary, hindlimb (S1HL)	+/+
Somatosensory, primary, trunk (S1Tr)	+/+ <sup>a</sup>
Somatosensory, secondary (S2)	+/+ <sup>a</sup>
Temporal association (TeA)	+/+ <sup>a</sup>
Visual, primary (V1)	+/+
Visual, secondary (V2)	+/+
<i>Subcortical regions</i>	
Amygdala, central n. (CeA)	+/+
Amygdala, lateral n. (LaA)	+/+ <sup>a</sup>
Amygdalostriatal transition area (ASt)	+/+
Caudate-putamen, dorsal (CPu)	+/+ <sup>a</sup>
Caudate-putamen, lateral (CPu)	-/-
Hippocampus, CA1, posterior	-/-
Hypothalamus, lateral (PeFLH, PLH)	-/-
Inferior colliculus (IC)	+/+
Parabrachial n. (PBN)	-/-
Periaqueductal gray, (PAG)	-/- <sup>a</sup>
Pontine reticular nucleus, caudal (PnC)	-/-
Red nucleus (RN), parabrachial n. (PaR)	-/-
Substantia nigra (SN)	-/-
Superior colliculus (SC)	-/-
Thalamus, ventroposterior complex (ventroposterior lateral, ventroposterior medial, parvocellular ventral posterior nuclei, VPL, VPM, VPPC)	-/-
Thalamus, parafascicular (PF), posterior (Po), ventromedial nuclei, (VM)	-/-
Trigeminal nucleus, sensory, lateral (Pr5VL)	-/-

Significant increases or decreases are noted with '+' and '-', respectively, for the left and right hemispheres. Significance is shown at the voxel level ( $P < 0.05$ ) for clusters  $>100$  contiguous voxels.

<sup>a</sup>Significance is shown at the voxel level ( $P < 0.01$ ). Shaded cells in addition show a correlation between regional cerebral blood flow (rCBF) with EMG and rCBF with behavioral pain score. Abbreviations are taken from the Paxinos and Watson rat atlas [59].